
Figures and figure supplements

Human and nonhuman primate meninges harbor lymphatic vessels that can be visualized noninvasively by MRI

Martina Absinta *et al*

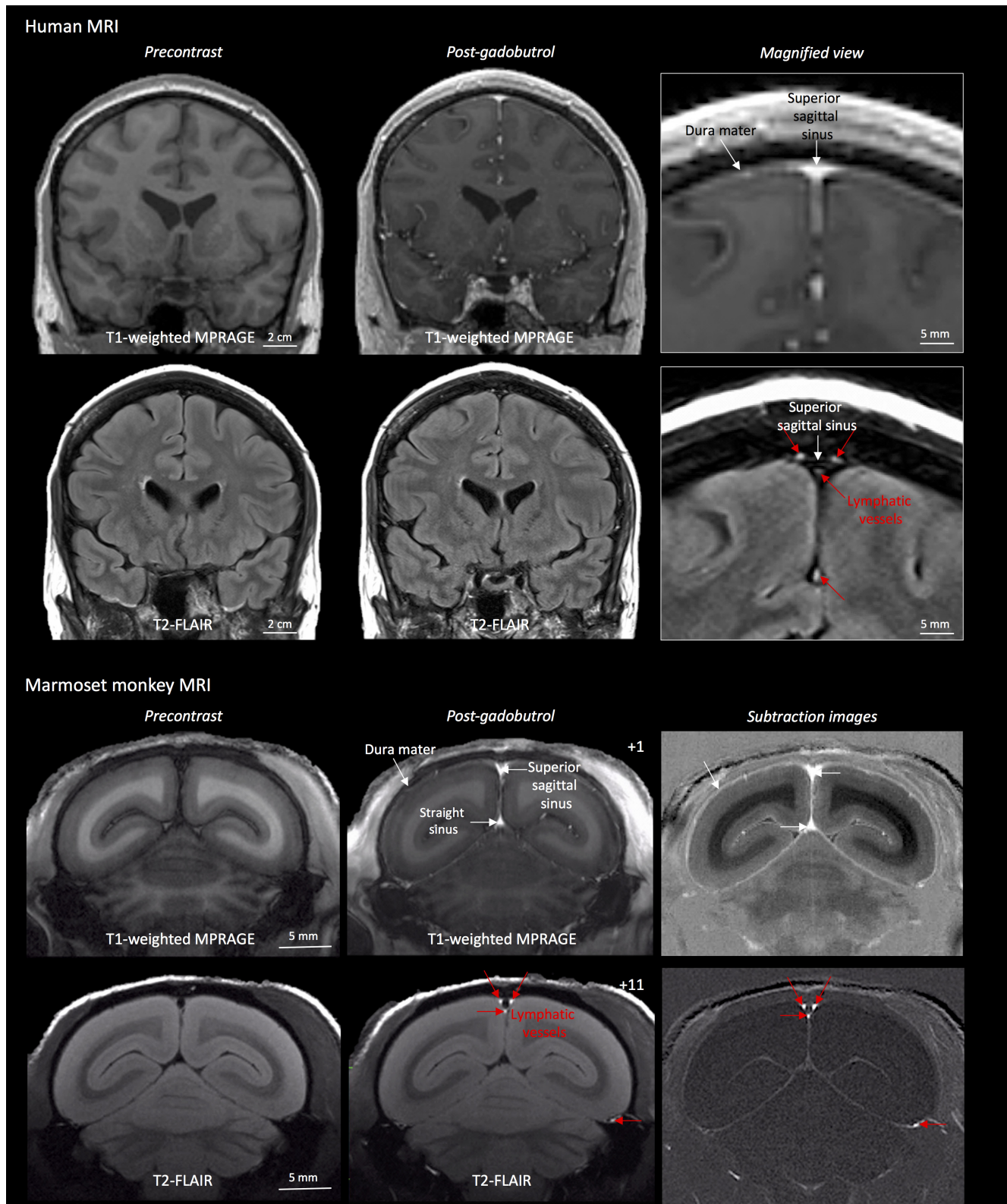


Figure 1. MRI-visualization of dural lymphatic vessels in human and nonhuman primates. In both species, conventional post-gadobutrol coronal T1-weighted MRI is unable to discriminate lymphatic vessels due to diffuse physiological enhancement of the dura (arrows) and blood vessels, including

Figure 1 continued on next page

Figure 1 continued

the superior sagittal sinus and straight sinus (arrows). On post-gadobutrol coronal T2-FLAIR and subtraction images, the dura does not enhance, and lymphatic vessels (red arrows), running alongside the venous dural sinuses and within the falx cerebri, can be appreciated. Numbers refer to minutes after the intravenous administration of gadobutrol.

DOI: <https://doi.org/10.7554/eLife.29738.003>

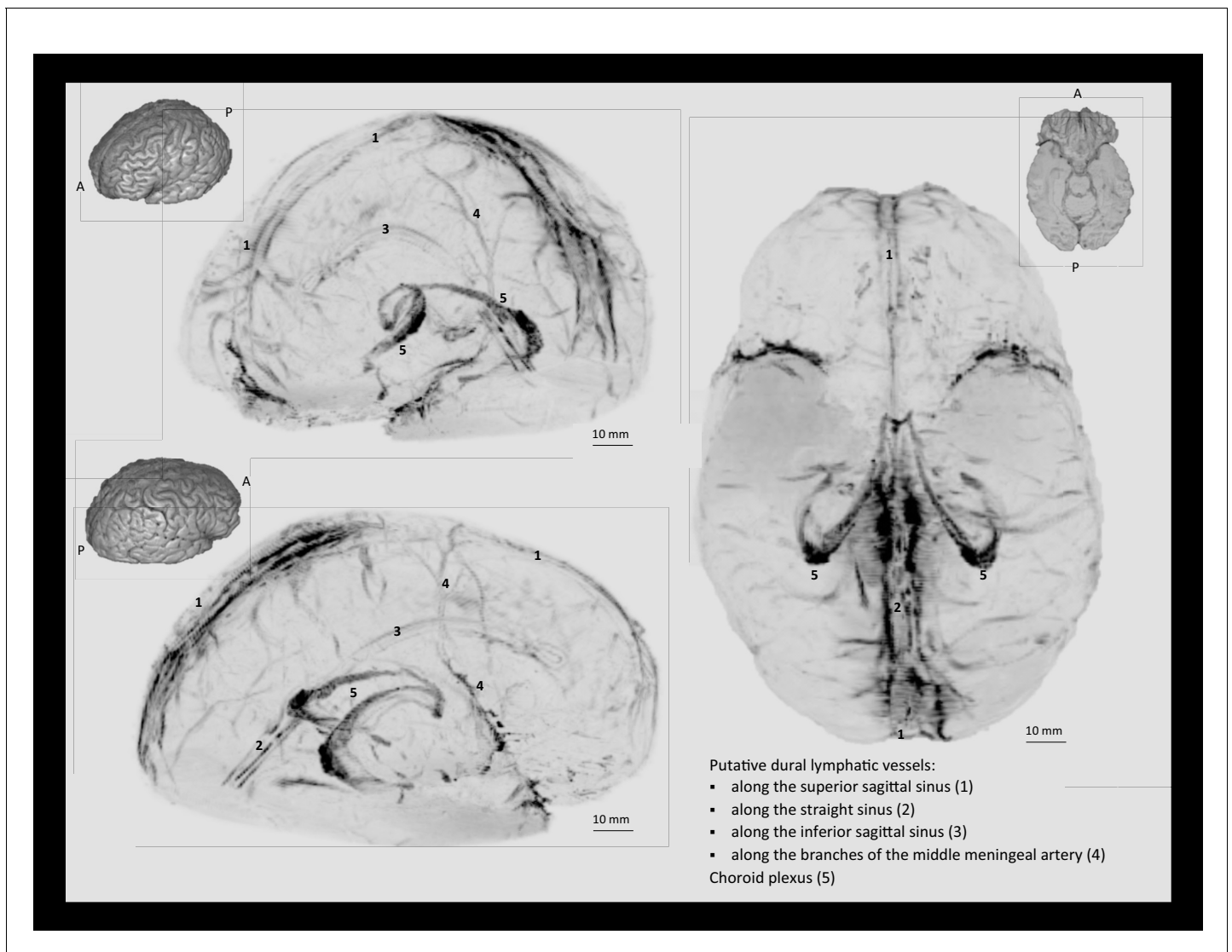


Figure 1—figure supplement 1. 3D rendering of human dural lymphatics. 3D rendering of putative dural lymphatics (black) in a 47 year old woman, derived from skull-stripped subtraction T1-black-blood images (same case as in **Video 1**). Thumbnails are 3D renderings of the brain parenchyma to aid visualization of image orientation.

DOI: <https://doi.org/10.7554/eLife.29738.004>

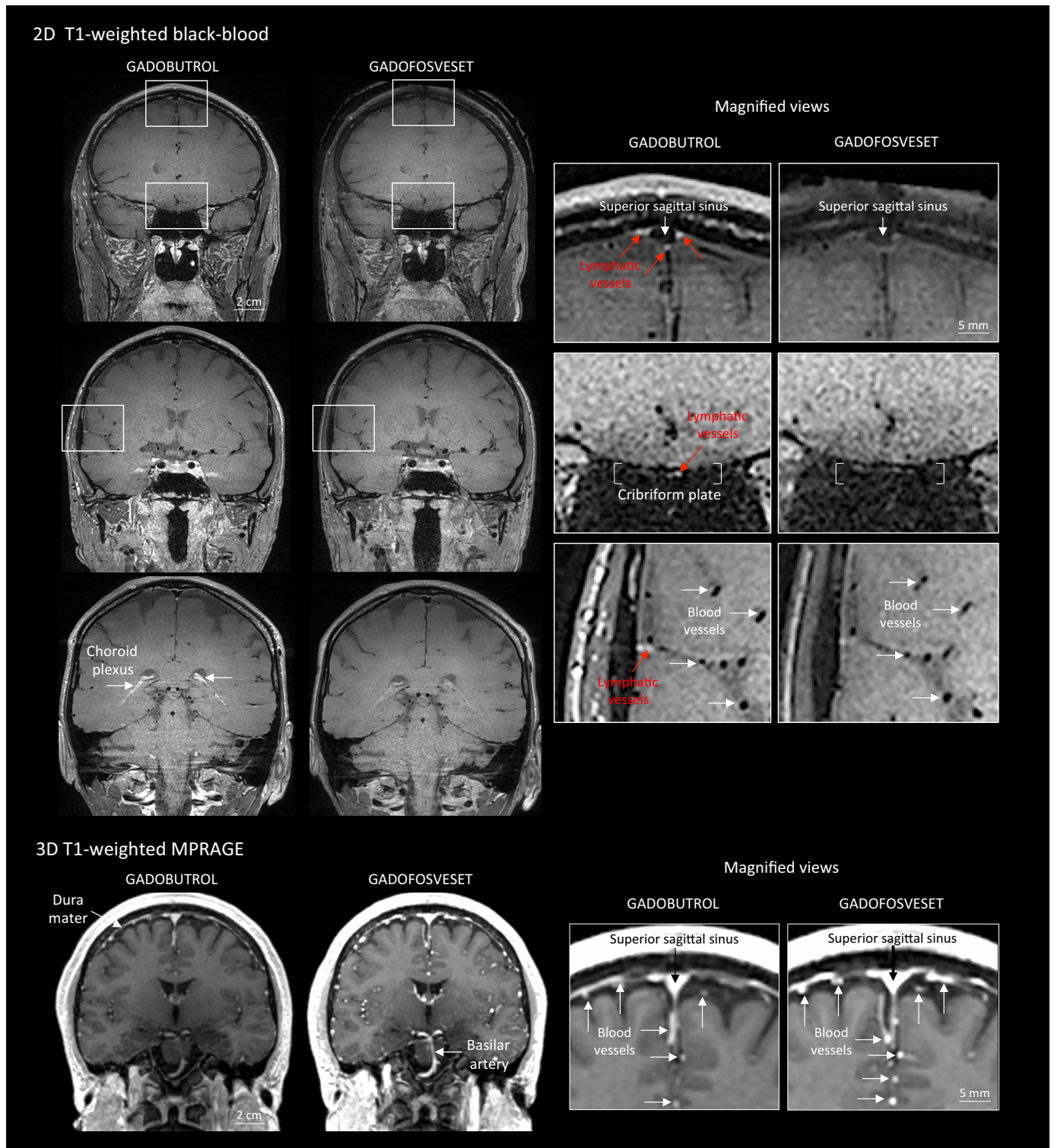


Figure 2. Gadobutrol vs. gadofosveset in MRI-visualization of dural lymphatic vessels. Coronal T1-weighted black-blood images were acquired after intravenous injection of two different gadolinium-based contrast agents (31 min after gadobutrol and 42 min after gadofosveset), during two MRI sessions separated by one week. Dural lymphatics (red arrows in magnified view boxes) were better discerned using gadobutrol (standard MRI contrast agent, which readily enters the dura) compared to gadofosveset (serum albumin-binding contrast agent, which remains largely intravascular) and were

Figure 2 continued on next page

Figure 2 continued

localized around dural sinuses, middle meningeal artery, and cribriform plate (white arrows). Notably, the choroid plexus (white arrows) enhanced less with gadofosveset than gadobutrol, whereas meningeal and parenchymal blood vessels (both veins and arteries) did not enhance with any contrast agent and appeared black. On conventional T1-weighted MPRAGE images, meningeal and parenchymal blood vessels enhanced with both contrast agents, more clearly with gadofosveset.

DOI: <https://doi.org/10.7554/eLife.29738.005>

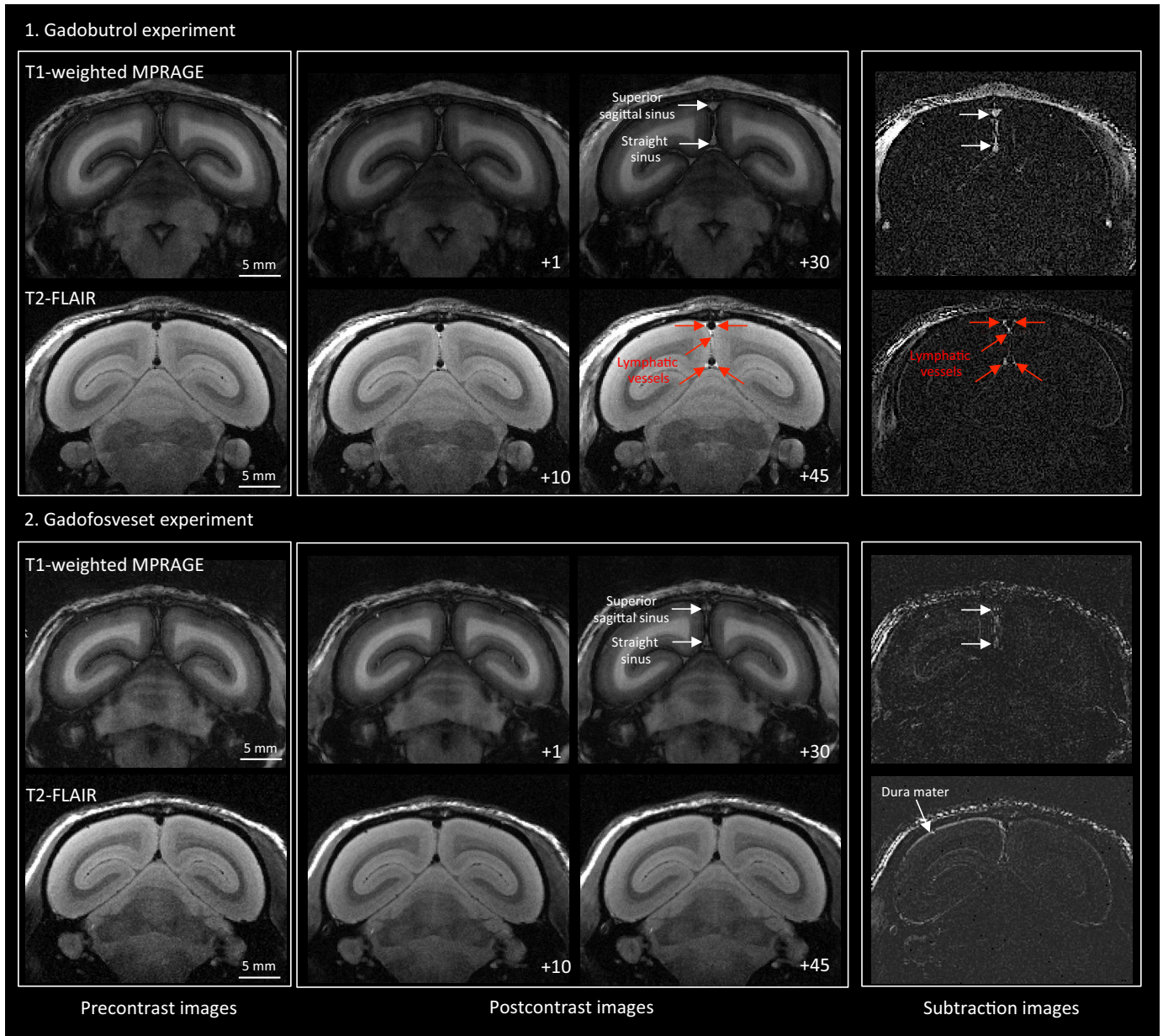


Figure 2—figure supplement 1. MRI visualization of dural lymphatic vessels in a healthy marmoset with different contrast agents. In an 11-year-old healthy common marmoset, high-resolution ($150 \times 150 \mu\text{m}$ in-plane) coronal T1-weighted MPAGE and T2-FLAIR were acquired before and at different time points after the injection of two different contrast agents (single dose of gadobutrol and gadofosveset), a week apart. (1) Gadobutrol experiment. Dural lymphatic vessels are discriminated on postcontrast T2-FLAIR and on subtraction images (post vs. precontrast images), but not on postcontrast 3D T1-weighted MPAGE. (2) Gadofosveset experiment. Gadofosveset, which binds serum albumin and therefore remains largely inside blood vessels (white arrows on postcontrast T1-MPAGE and subtraction images), even in tissues (such as the dura mater) that lack a blood-brain barrier, is FDA-approved for magnetic resonance angiography. Dural lymphatic vessels are not visible on post-gadofosveset T2-FLAIR and relative subtraction images, even on delayed acquisition (45 min after injection), despite preserved enhancement of the dural venous sinuses. Numbers refer to minutes after intravenous administration of the contrast agent.

DOI: <https://doi.org/10.7554/eLife.29738.006>

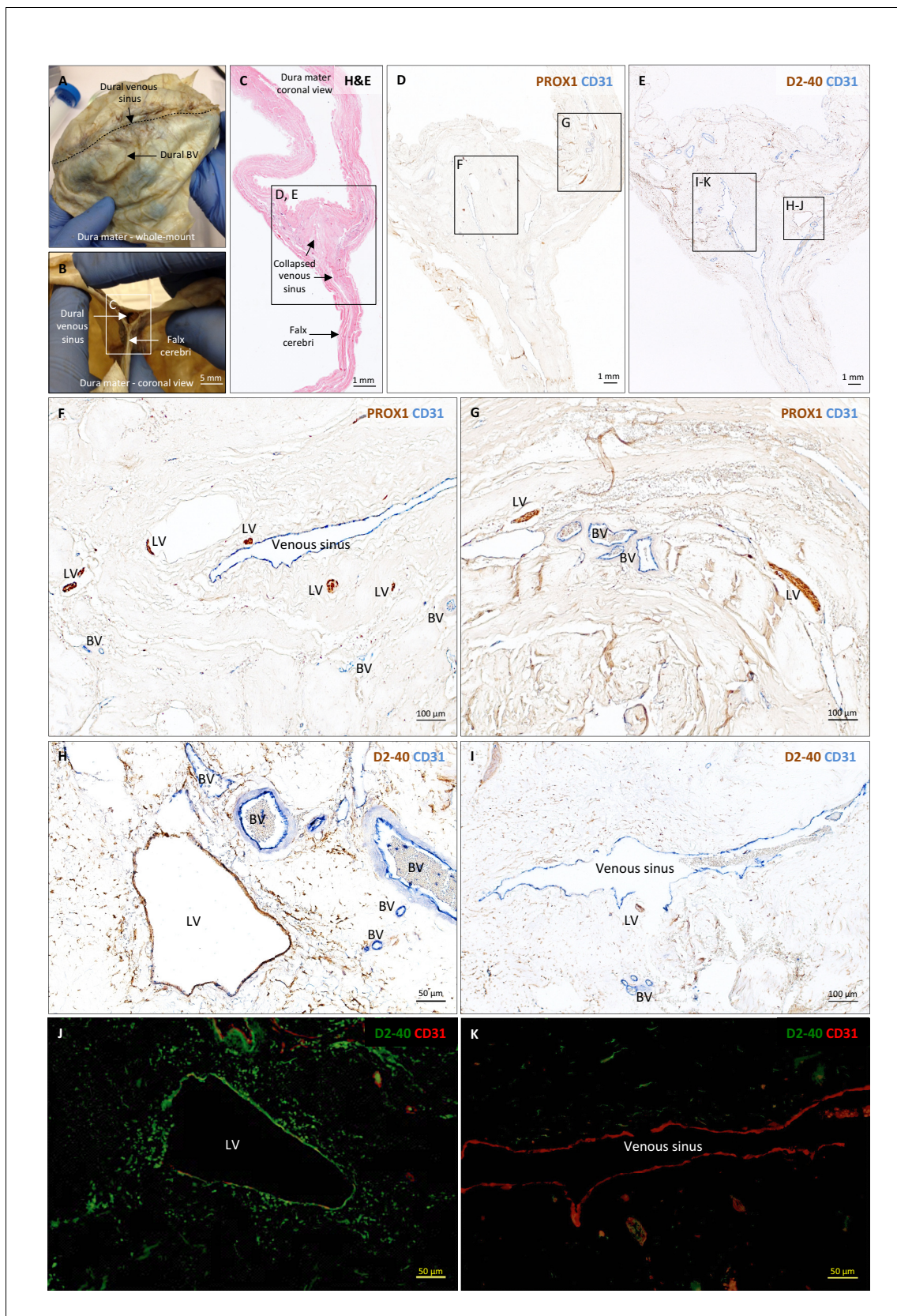


Figure 3. Histopathology of human dural lymphatic vessels. (A–B) Whole-mount and coronal views of the human dura mater before sampling for histological analysis. The dotted line in A shows where the superior sagittal sinus runs within the dural layers. (C) Coronal section of human dura stained with H&E. Figure 3 continued on next page

Figure 3 continued

with H and E to highlight anatomical features of interest, including the falx cerebri and the dural venous sinus. Note the distortion of the dura after paraffin embedding in comparison to B. (**D, F, G**) Within the dura mater, lymphatic and blood vessels can be differentiated using double immunostaining for PROX1 (a transcription factor involved in lymphangiogenesis, nuclear staining) and CD31 (a vascular endothelial cell marker). (**E, H–K**) Similarly, lymphatic and blood vessels can be differentiated using immunohistochemical (**E, H, I**) and immunofluorescent (**J, K**) double staining for podoplanin (D2-40, endothelial membrane staining) and CD31. Red blood cells are seen within blood vessels, but not within lymphatic vessels. Insets (**F–I**) were rotated relative to the original figures in D and E. *Abbreviations:* H and E: hematoxylin and eosin; LV: lymphatic vessels; BV: blood vessels.

DOI: <https://doi.org/10.7554/eLife.29738.007>

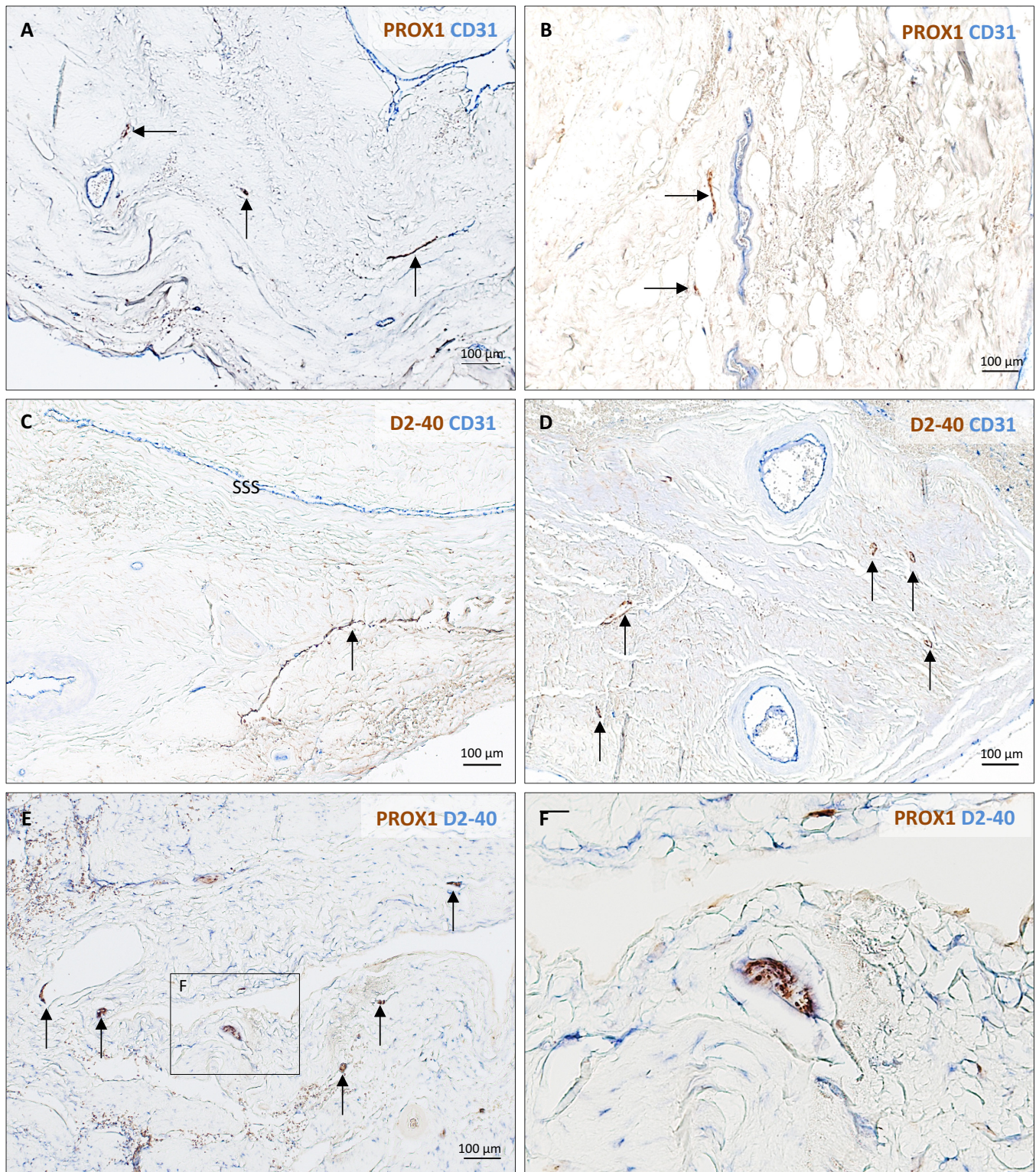


Figure 3—figure supplement 1. Histopathology of human dural lymphatic vessels. Lymphatic vessels (brown, arrows) in different samples of human dura mater visualized with double immunostaining (PROX1/CD31, D2-40 podoplanin/CD31, PROX1/D2-40 podoplanin).

DOI: <https://doi.org/10.7554/eLife.29738.008>

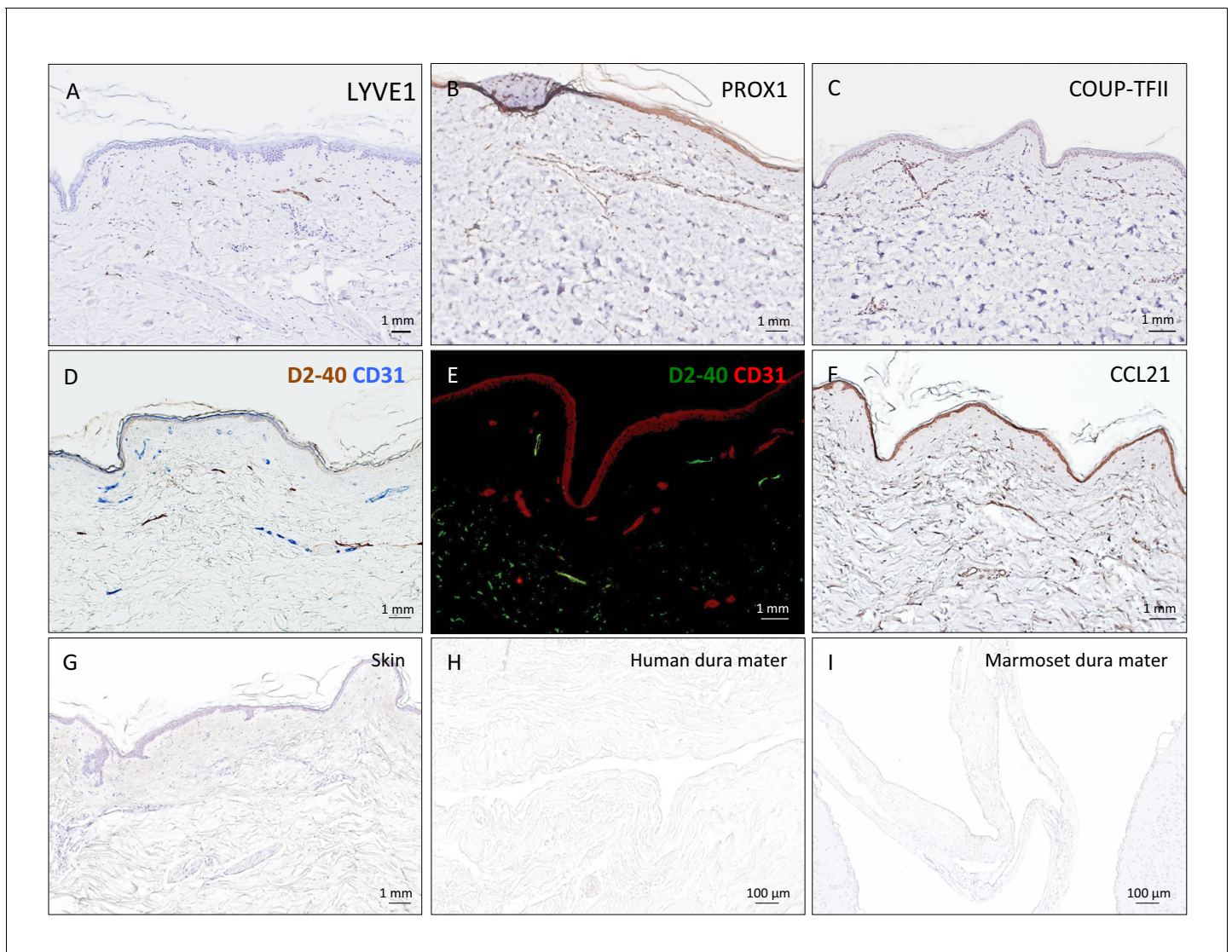


Figure 3—figure supplement 2. Positive and negative control staining for lymphatic vessels. (A–F) 5 μm paraffin sections of the human skin were implemented as positive controls for lymphatic endothelium cell marker assessment. (G–I) Negative control staining (only secondary antibodies, DAB development, and hematoxylin) of 5 μm paraffin sections of human skin, human dura mater, and marmoset brain, respectively. No background staining or nonspecific binding was seen in any tissue.

DOI: <https://doi.org/10.7554/eLife.29738.009>

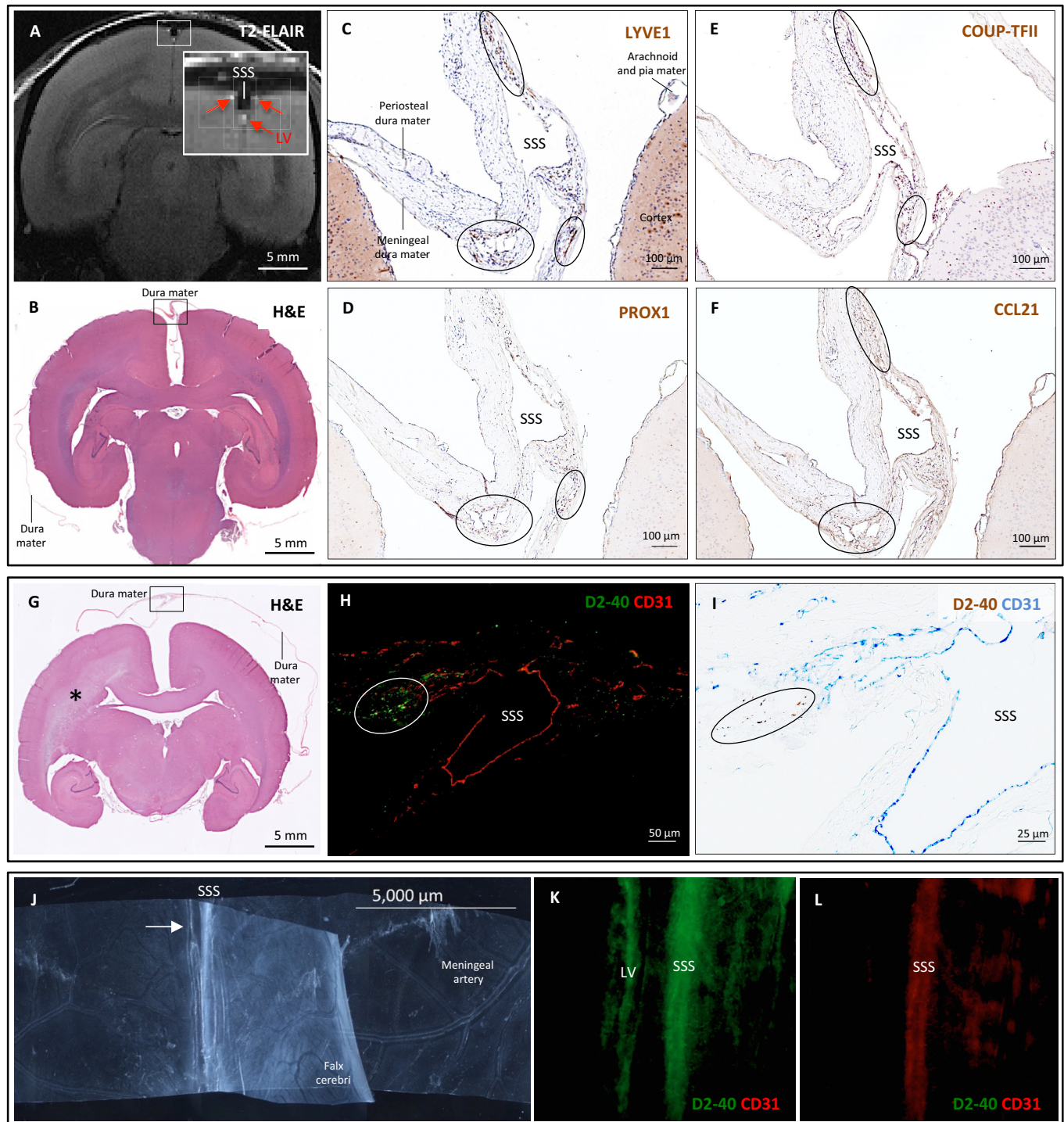


Figure 4. Histopathology of dural lymphatic vessels in common marmosets. MRI-histopathological correlation in a 4.4-year-old marmoset (A–F). (A, B) Postcontrast coronal T2-FLAIR showing three enhancing lymphatic vessels within the dura, and corresponding H and E section for anatomical reference (area of interest in the box). (C–F) Three clusters of cells (circles), surrounding the SSS and positive for lymphatic endothelial cell markers, correspond to the three enhancing areas seen on MRI (A). LYVE-1 is a lymphatic endothelial cell marker (membrane staining), PROX1 and COUP-TFII are transcription factors involved in lymphangiogenesis (nuclear staining), and CCL21 is a chemokine implicated in lymphatic transmigration. Higher magnifications are shown in **Figure 4—figure supplement 1**. 10.3-year-old marmoset (G–I). (G) H and E coronal section showing the brain parenchyma, meninges, and dura mater. (H, I) IHC staining for D2-40 and CD31 showing membrane staining. (J–L) High-magnification views of the SSS and meningeal artery. Figure 4 continued on next page

Figure 4 continued

area of interest for lymphatics for anatomical reference (box). This animal did not recover after undergoing general anesthesia for blood tuberculosis testing, and at necropsy a stroke was identified in one hemisphere (asterisk). (H-I) Lymphatic (circles) and blood vessels were differentiated using double staining for podoplanin (D2-40, endothelial membrane staining) and vascular endothelial cell marker (CD31), respectively. 3.7-year-old marmoset (J-L). (J) Whole-mount of the marmoset dura, including the SSS. The high level of vascularization of the dura can be appreciated. The arrow indicates the area shown in K and L. (K, L) Double staining for podoplanin D2-40 for lymphatics, and CD31 for vascular endothelial cells, show the presence of a linear vascular structure parallel to the SSS, positive for podoplanin D2-40 but not CD31. The SSS is positive for both markers, probably because of antibody entrapment during immunofluorescence staining of the whole-mount dura. Abbreviations: H and E: hematoxylin and eosin; LV: lymphatic vessels; SSS: superior sagittal sinus.

DOI: <https://doi.org/10.7554/eLife.29738.011>

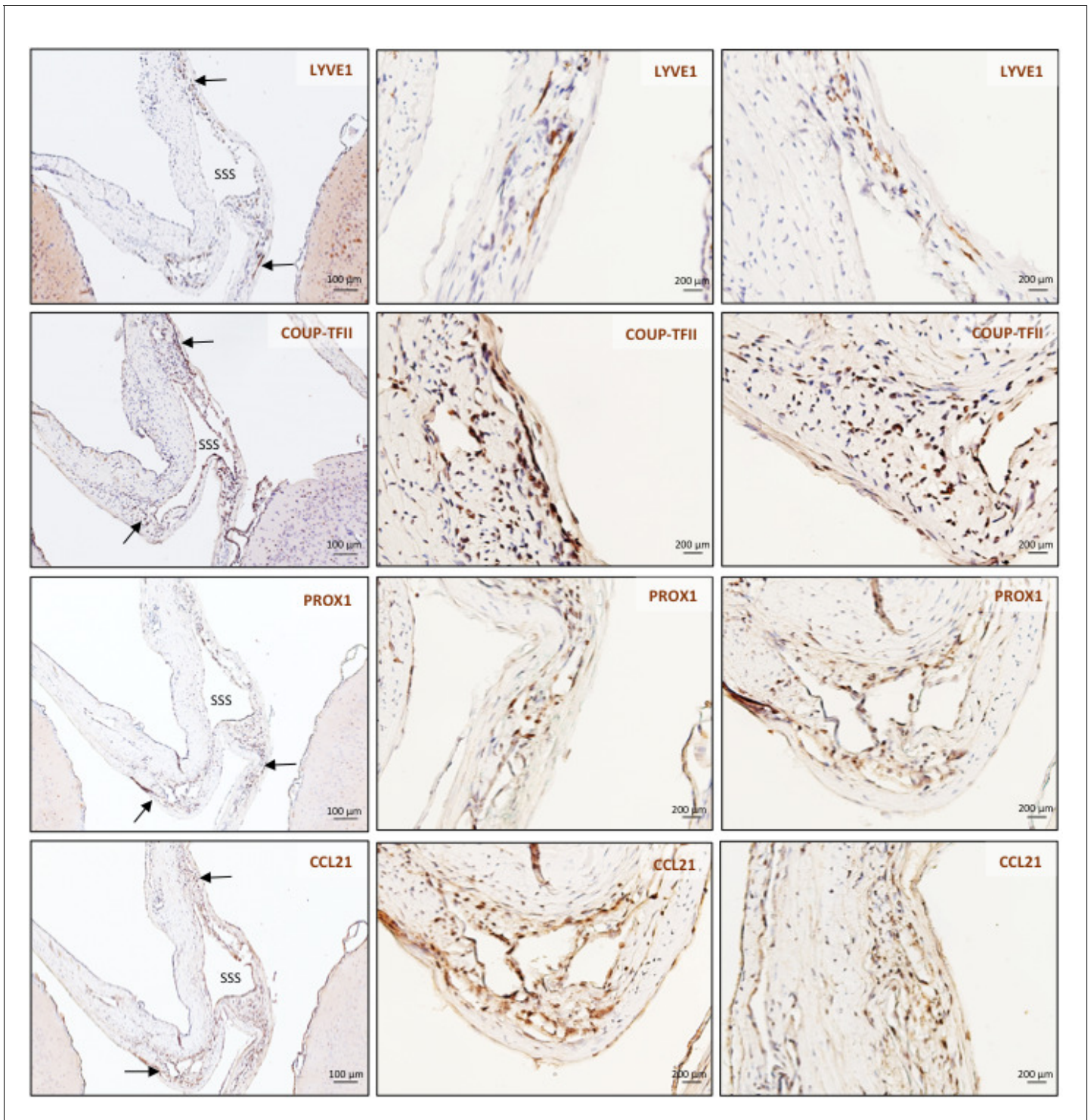


Figure 4—figure supplement 1. Histopathology of marmoset dural lymphatic vessels. High magnification of insets C-F from **Figure 4**.

DOI: <https://doi.org/10.7554/eLife.29738.012>